forests

MDPI

Article

Mycorrhizal Fungi Synergistically Promote the Growth and Secondary Metabolism of *Cyclocarya paliurus*

Tingting Zhao †, Bangyou Yu †, Mengjia Zhang, Shuying Chen and Bo Deng *

School of Forestry and Landscape Architecture, Anhui Agricultural University, Hefei 230036, China
* Correspondence: bodeng@ahau.edu.cn
† These authors contributed equally to this work.

Abstract: *Cyclocarya paliurus* has traditionally been used as medicine or a nutraceutical food. This study aims at investigating whether the growth and secondary metabolism of *C. paliurus* could be simultaneously promoted by inoculating with mycorrhizal fungi, and if so, to uncover the underlying regulatory mechanism. A mycorrhizal microbial inoculum, consisting of the superficial layer fine roots and rhizosphere soil collected from the natural forest of *C. paliurus*, was used to infect aseptic seedlings of *C. paliurus*. Roots of aseptic seedlings were successfully infected by mycorrhizal fungi with a 59.7% colonization rate. For mycorrhizal seedlings of *C. paliurus*, the induced endogenous auxin, net photosynthetic rate, nitrogen absorption, and growth-related genes resulted in a significantly higher growth and biomass accumulation. In addition, a systemic defense response was observed in response to mycorrhizal fungal colonization, such that jasmonic acid biosynthesis and signaling were induced and the biosynthesis of secondary metabolites and antioxidant systems were up-regulated. The improved growth and accumulation of secondary metabolites ultimately facilitated the yield of health-promoting substrates per plant. Overall, mycorrhizal fungal colonization had a significant positive effect both on growth and production of secondary metabolites in *C. paliurus*. The results can provide the basis for overcoming the limitation of soil nutrient regulation in cultivation practice and offering a simpler alternative to improve the quality of medicinal plants.

Keywords: *Cyclocarya paliurus*; mycorrhizal fungi; growth; flavonoid; triterpenoid

Citation: Zhao, T.; Yu, B.; Zhang, M.; Chen, S.; Deng, B. Mycorrhizal Fungi Synergistically Promote the Growth and Secondary Metabolism of *Cyclocarya paliurus*. *Forests* **2022**, *13*, 2188. https://doi.org/10.3390/f13122188

Academic Editor: Timothy A. Martin

Received: 26 July 2022
Accepted: 16 December 2022
Published: 19 December 2022

1. Introduction

Cyclocarya paliurus, which is widely distributed in sub-tropical regions of China, belongs to the Juglandaceae family. The leaves of *C. paliurus* have long been used to make traditional Chinese medicine and have also been used as a functional food resource [1]. Previous studies showed that the high content of physiological active substances in the leaves of *C. paliurus*, such as flavonoids and triterpenoids, can protect against a range of diseases, including lowering blood lipids, anti-oxidation, and immune-modulation [2–4]. The main cultivating target of medicinal *C. paliurus* is to improve the biosynthesis and accumulation of secondary metabolites through cultural operations and environmental regulation. However, little information is available about the efficient cultivation technology of *C. paliurus* plantation in practice.

In the artificial cultivation practice of medicinal plants, we pay great attention to the balance between quality and yield, which is related not only to the quality of raw materials but also to obtain the greatest yield of target products. Quality is associated with the biosynthesis and accumulation of secondary metabolites such as flavonoids and terpenoids, while yield is associated with plant growth and biomass accumulation. Our previous studies found that the high level of inorganic NPK fertilizer (15% N, 15% P_2O_5, and 15% K_2O) application inhibited the accumulation of flavonoids, and the highest flavonoid production per plant was achieved in intermediate fertilization treatment [5]. Later studies further proved that flavonoids can be largely biosynthesized only when plant growth was

repressed under low nutrient availability, and a large amount of stored carbohydrates can provide carbon skeleton and energy for flavonoid biosynthesis [6,7]. With regards to the effects of phosphate availability on flavonoid accumulation, our recent study also found that the low level of phosphorus improved flavonoid accumulation, while plant growth was repressed [8]. These results suggested that low availability of nutrients such as nitrogen and phosphorus led to the biosynthesis and accumulation of flavonoids in *C. paliurus*, while resulted in an inhibition of plant growth. Thus, there is a trade-off between the biosynthesis of secondary metabolites and plant growth, which limits the production of medicinal plants with the goal of obtaining the greatest yield of targeted secondary metabolites. Therefore, the effective way to improve the yield per unit area of medicinal plants is to promote the biosynthesis of secondary metabolites without reducing growth through appropriate measures in cultivation practice.

In terrestrial ecosystems, more than 90% of vascular plants have a pervasive symbiotic association between the plant roots and mycorrhizal fungi; plants provide photosynthates for mycorrhizal fungi and, in return, fungi promote the absorption of water and soil nutrients, and improve the resistance of host plants to biotic and abiotic stresses [9]. As a result, mycorrhizal fungi have a wide range of growth-promoting effects, and these dhave been applied in agri-forestry production. Recently, it has been found that mycorrhizal fungi can also promote terpenoid biosynthesis in plants. The biosynthesis of artemisinin in *Artemisia annua* and stevioside in *Stevia rebaudiana* was induced by mycorrhizal fungi by upregulating the transcription of downstream genes of the dedicated biosynthetic pathway [10,11]. Therefore, the application of mycorrhizal fungi may be a potentially effective approach to promote both the growth and biosynthesis of secondary metabolites, and ultimately facilitate the harvest yield of medicinal plants. However, less information is available about the promoting-effects of mycorrhizal fungi both on growth and secondary metabolism in the same plant. More recently, Sheteiwy et al. proved that the growth and flavonoid accumulation of soybean plant can be synergistically promoted through inoculation of specific mycorrhizal fungi [12]. Therefore, it is very important to explore the effects of mycorrhizal fungi on the growth and secondary metabolism of *Cyclocarya paliurus*, and its regulatory mechanisms for the efficient production of medicinal plants.

In the process of infecting plant roots, mycorrhizal fungi first decompose and break through the epidermal cells of roots, and the mycelium penetrates into the intercellular spaces or cells to form symbiotic structures such as Hartig net and arbuscules, which can induce the defense response of host plants against fungal infection [13]. During the formation of mycorrhizal symbiosis in roots of *Populus trichocarpa*, the infection of *Laccaria bicolor* induced jasmonic acid release by plant cells, which was subsequently sensed by the COI1 protein, and eventually induced the defense response of plants. On the other hand, however, the *MiSSP7* gene in plants can inhibit the defense response induced by fungal infection to a certain extent, thus enabling mycorrhizal fungi to form a symbiotic association with plants [14]. Jasmonates (jasmonic acid, methyl jasmonate, etc.) are phytohormones and signaling molecules associated with plant injury, which have been extensively studied during mycorrhizal formation. The local and systemic damage signals will be triggered after plants suffer mechanical damage, inset feeding or fungus colonization, and ultimately form jasmonates through a multi-step reaction [15,16]. Exogenous jasmonates can also induce the expression of plant defense genes, trigger chemical defense, and stimulate responses similar to mechanical damage and insect feeding, such as inducing protease inhibitors, peroxidase, and even the formation of physical defense structures [17]. The biosynthesis and accumulation of secondary metabolites is one of the important chemical defense strategies in plants. For example, flavonoids accumulate in response to diverse biotic and abiotic stresses and function as reactive oxygen species scavengers to reduce oxidative damage [18]. Terpenoids play an important role in enhancing plant resistance to disease, preventing herbivores from feeding and maintaining a reciprocal association with other biological groups [19,20].

In this study, we wanted to explore whether the growth and secondary metabolism of *C. paliurus* could be promoted simultaneously by inoculating with mycorrhizal fungi, and if so, to uncover the underlying regulatory mechanism. The growth, biomass accumulation, content and yield of secondary metabolites, and global transcriptional profile of *C. paliurus* were investigated. This knowledge will provide the basis for overcoming the limitations of soil nutrient regulation in cultivation practice and offer a simpler alternative to improve the quality of medicinal plants.

2. Materials and Methods

2.1. Plant Material and Experimental Design

Seeds of *C. paliurus* were collected from natural forests (a selected single tree) of Anji (Zhejiang, China) in late October 2019. The collected seeds were first subjected to chemical scarification, followed by exogenous gibberellin A3 (GA3) treatments, and then stratification treatments using a method described by Fang et al. [21]. After stratification treatment for 3 months, the germinated seedlings were transplanted to containers which were filled with the sterilized culture substrate of peat soil-perlite (*v*/*v* = 1/1).

In May 2020, the cluster-distributed natural forest of *C. paliurus* in Wanfoshan, Anhui, China, was selected, and the well-grown large trees of *C. paliurus* were designated as the target trees for mycorrhizal collection. The superficial layer (0–30 cm) fine roots and the soil on the root surface (rhizosphere soil) were collected. The method described by Zhang et al. was used to prepare the mycorrhizal microbial inoculum [22]. In brief, the fine roots were cut into root segments of approximately 1 cm, which were subsequently mixed evenly with rhizosphere soil, and dried naturally. At the end of May 2020, the aseptic seedlings (seedlings grown on sterilized substrates to ensure that their roots are free of mycorrhizal fungi) of *C. paliurus* that had a uniform growth (possess similar plant height and ground diameter) were selected and re-transplanted to the experimental containers (12 cm in diameter, and 18 cm in height). These were filled with topsoil collected from the nursery garden, which had a pH value of 5.9, total organic matter of 89.8 g/kg, total nitrogen of 11.54 g/kg, total phosphorus of 1.18 g/kg, total potassium of 6.66 g/kg, total calcium of 3.97 g/kg, and total magnesium of 3.43 g/kg. In this study, 20 g mycorrhizal microbial inoculum was added to the root area for infecting the aseptic seedlings of *C. paliurus*. In contrast, the mycorrhizal microbial inoculum sterilized by autoclaving was characterized as the control. Three replicates were contained in each treatment, with each replicate consisting of 10 seedlings. All of the seedlings were grown in a controlled phytotron with 620 μmol $m^{-2} \cdot s^{-1}$ light intensity, a 12 h photoperiod, a 25 °C/15 °C diurnal/night temperature and a constant relative humidity of 65%. The fresh fine roots were used for observing the infection rate of mycorrhizal fungi and for molecular identification of fungal species diversity. After 5 months of inoculation, the fine roots of *C. paliurus* seedlings were collected for colonization rate investigation.

2.2. Observation on Colonization of Mycorrhizal Fungi

In order to observe the colonization of mycorrhizal fungi, the white to yellowish radicles from the natural large trees and/or from the test seedlings of *C. paliurus* were collected. The sampled radicles were subjected to flushing with water, followed by trypan blue histochemical staining as described by Massenssini et al. [23]. In brief, the radicles were divided into segments of about 1 cm long, and then the root segments were softened with 20% KOH solution in a water bath at 90 °C for 30 min, and finally decolorized with alkaline H_2O_2 solution at room temperature for 2 h. The pretreated root segments were stained in a 0.05% Trypan Blue–lactic acid solution in a boiling water bath for 10 min. After decolorization with distilled water, the colonization of mycorrhizal fungi in root segments was observed by using a light microscope (Axiosope5, Carl Zeiss AG, Jena, Germany), and the colonization rate was calculated.

2.3. Measurements of Plant Growth, Biomass, Root Traits and Photosynthetic Rate

The height and ground diameter of seedlings were measured monthly from July to October, while biomass measurements were performed at the end of October 2020. For day mass investigation, the seedlings of *C. paliurus* were separated into root, stem and leaf, and all the components were dried at 70 °C and weighed. Total dry mass was calculated as the sum of the root, stem and leaf dry weight. After the determination of dry mass, the samples were ground into powder for storage. In order to evaluate the effects of mycorrhizal fungi inoculation on root traits, the length of the taproot and lateral root, and the number of lateral roots were investigated at the end of October.

At the beginning of October, the net photosynthesis rate was measured during 9:00–11:00 on a sunny day. Three seedlings per replicate were selected, the fully developed leaflets on the 4-th compound leaf below the apex on each selected seedling were marked, and the measurements were performed by using a Li-6400XT photosynthetic system (LI-COR, Inc., Lincoln, NE, USA).

2.4. Measurement of Phytohormones

The fresh leaves of *C. paliurus* were sampled at the end of October, and the phytohormones were isolated with an isopropanol–water–hydrochloric acid solution. The levels of *phytohormones* such as jasmonates and auxin in leaves of *C. paliurus* were targeted for metabolite assay by high performance liquid chromatography coupled with mass spectrometry. The mobile phases were composed of methanol solution of 0.1% formic acid (*v/v*, A) and ultrapure water solution of 0.1% formic acid (*v/v*, B) with a flow rate of 1.0 mL/min. The gradient elution program was as follows: 0–1 min, 20% A; 1–9 min, 20%–80% A; 9–10 min, 80% A; 10–11 min, 80%–20% A; 11–15 min, 20% A. The peak identifications were carried out on an SCIEX-6500Qtrap (MS/MS) mass spectrometer system, and the MS system was operated in negative ionization modes with the mass scan range between *m/z* 52–360. The mass spectral parameters were: a gas flow of 10 L/min, gas temperature of 400 °C, capillary voltage of 4500 V, cone voltage of 100 V, collision voltage of 60 V, and nebulizer pressure of 70 psi. The standards of jasmonic acid, jasmonic acid-isoleucine, and 3-indoleacetic acid (Sigma-Aldrich Inc., St. Louis, MO, USA) were used to obtain an external calibration curve.

2.5. Measurement of Mineral Nutrient

In order to measure the contents of mineral nutrients in different organs of *C. paliurus*, the above crushed samples were used. The total contents of carbon (C) and nitrogen (N) were determined by using an elemental analyzer system (Euro Vector EA 3000, Pavia, Italy). The total content of potassium (K), calcium (Ca) and magnesium (Mg) was determined using an atomic absorption spectrophotometer (AA-6300, Shimadzu Cor., Kyoto, Japan) after digesting with nitric acid-perchloric acid, while the total content of phosphorus (P) was determined using flow injection analysis (Futura, AMS Alliance, Mumbai, France).

2.6. Extraction and Determination of Triterpenoids and Flavonoids

To remove the fat-soluble components, approximately 0.3 g of sample was placed in a 250 mL Soxhlet extractor and extracted with petroleum ether at reflux for 4 h in an 80 °C water bath. Then, 20 mL of 70% ethanol solution was used to extract the triterpenoids and flavonoids from the samples by ultrasonic-assisted extraction. The combined extracts were evaporated to near dryness, and the residue was repeatedly washed with methanol and fixed to 10 mL as samples for the determination of triterpenoids and flavonoids. Total flavonoid content was determined by using a colorimetric method described by Bao et al. [24]. Rutin (National Institute for the Control of Pharmaceutical and Biological Products, Beijing, China) was used as the external standard to calculate the concentration of flavonoid in the extracts, and the total flavonoid content expressed as milligram rutin equivalent per gram of dry weight (mg/g). To determine the content of total triterpenoid, a colorimetric method with minor modifications performed at a wavelength of 560 nm

according to Fan and He was used [25]. Total triterpenoid concentration in the extracts was determined by referencing to a standard oleanolic acid (National Institute for the Control of Pharmaceutical and Biological Products, Beijing, China) curve.

Individual flavonoids and triterpenoids were isolated and identified by high performance liquid chromatography coupled with quadrupole time-of-flight mass spectrometry (HPLC-Q-TOF-MS) according to Cao et al. [26]. In brief, a Waters e2695 Alliance HPLC system (Waters Corp., Milford, CT, USA), consisting of a water separation unit, an auto sampler, a gasket-cleaning system, a column heater, an online degasser, a Waters 2489 ultraviolet detector, and an Empower 3 data-processing system. The mobile phases were composed of acetonitrile solution of 0.01% formic acid (*v/v*, A) and aqueous solution of 0.01% formic acid (*v/v*, B) with a flow rate of 1.0 mL/min. The gradient elution program was as follows: 0–13 min, 8%–19% A; 13–28 min, 19%–21% A; 28–42 min, 21%–50% A; 42–46 min, 50% A; 46–60 min, 50%–55% A; 60–64 min, 55%–56% A; 64–74 min, 56%–66% A; 74–90 min, 66%–85% A; 90–95 min, 85%–100% A; 95–100 min, 100% A. The peak identifications were carried out on an Agilent 6520 Q-TOF mass spectrometer system equipped with an electrospray interface, a diode array detector, and a Agilent Mass Hunter data acquisition and processing (version B. 04. 00). The MS system was operated in negative ionization modes with the mass scan range between *m/z* 100–1200. The mass spectral parameters were a gas flow of 10 L/min, gas temperature of 300 °C, capillary voltage of 4000 V, cone voltage of 100 V, collision voltage of 60 V, and nebulizer pressure of 30 psi.

2.7. RNA Extraction, Sequencing, and Differential Expression Analysis

The leaves of *C. paliurus* from mycorrhizal fungi inoculation and control seedlings were sampled at the end of October. A Picopure^{TM} RNA isolation Kit (Thermo Fisher Scientific, Waltham, MA, USA) was used to extract the total RNA from the callus, followed by RNA purification with RNase-free DNase I (TaKaRa, Dalian, China) and the tests of RNA degradation and contamination by using a 2% agarose gel electrophoresis. RNA concentration, purity and integrity were measured by using a Qubit 2.0 Fluorometer (Life Technologies, Carlsbad, CA, USA), a NanoPhotometer spectrophotometer (Implen, Westlake Village, CA, USA) and an Agilent 2100 analyzer (Agilent Technologies, Santa Clara, CA, USA), respectively. An Illumina HiSeq 2500 platform was used to construct the cDNA libraries. After transcriptome assembly and functional unigene annotation, differential expression and enrichment analysis was conducted. Briefly, the clean data was mapped back onto the assembled transcriptome, and the expression levels of unigenes were calculated based on the fragments per kilobase of transcript of transcript per million mapped reads (FPKM). Subsequently, the differentially expressed genes (DEGs) between the mycorrhizal fungi inoculation and control seedlings were selected. In this study, the DEGs were characterized as the genes with an absolute $\log_2$ (fold change) value ≥ 2 and a false discovery rate (FDR) ≤ 0.001. Based on the Walleniu' noncentral hypergeometric distribution, the GO enrichment analysis of DEGs was performed with Goseq R package. In addition, the KEGG pathway enrichment analysis of DEGs was conducted using KOBAS software for discerning the related biochemical and signal transduction pathways.

2.8. Identification of Fungal Microbiota Diversity in Roots

The well-growing large trees of *C. paliurus* were selected, and the superficial layer (0–30 cm) fine roots was sampled for identification of fungal microbiota diversity. The fine roots were firstly subjected to DNA extraction and examination, followed by PCR amplification and purification. In order to construct the rDNA-ITS library, primers were designed according to the conserved region of the ITS2 sequence (fITS7: 5′-GTGARTCATCGAATCTTTG-3′; ITS4: 5′-TCCTCCGCTTATTGATATGC-3′), and the universal connector and Barcode sequence were added to the primers [27]. After purifying, the PCR products were sequenced on a Miseq platform. The double-ended raw data were spliced based on overlap, and the high-quality data were obtained after chimera filtering. The sequences were

clustered with the 97% similarity, and the species annotation and diversity analysis were carried out according to the final OTU abundance and representative sequence.

2.9. Data Analysis

SPSS version 16.0 (SPSS Inc., Chicago, IL, USA) was used to perform the analysis of variance (ANOVA) and the significant differences among the treatments were calculated with Duncan's multiple-range test. All statistical analyses were performed at a 95% confidence level.

3. Results and Discussion

3.1. Variation in Colonization Rate

The fine roots collected from the natural forest of *C. paliurus* were firstly used for observing the colonization rate of mycorrhizal fungi and for molecular identification of fungal species diversity. The main mycorrhizal type was endophytic arbuscular mycorrhizal (AM) fungi, and a large number of typical AM fungi symbiotic structures were found through microscopic observation in fine roots of *C. paliurus*, such as arbuscules, septate hypha and vesicles (Figure 1a). The average colonization rate of mycorrhizal fungi on the fine root of natural large trees was 52.8% (Figure 1b). The results of molecular identification showed that a total of 11 genera of endophytic fungi with abundance greater than 0.5% were found in the fine roots of *C. paliurus*, including *Cnloridium*, *Cryptococcus*, *Cephalotheca*, *Glomus*, *Mortierella*, *Dactylaria*, *Penicillium*, *Archaeorhizomyces*, *Trichoderma*, *Mycena*, and *Lophiostoma* (Figure 1c). Among them, *Glomus* belongs to the arbuscular mycorrhizal fungi. In addition, the genera of mycorrhizal fungi with abundance less than 0.5% and those with no classification were combined into the Other group, and they made up more than 50% of the total fungal microbiota. These results indicated that endophytic fungi, including mycorrhizal fungi, are ubiquitous in fine roots of natural large trees of *C. paliurus*.

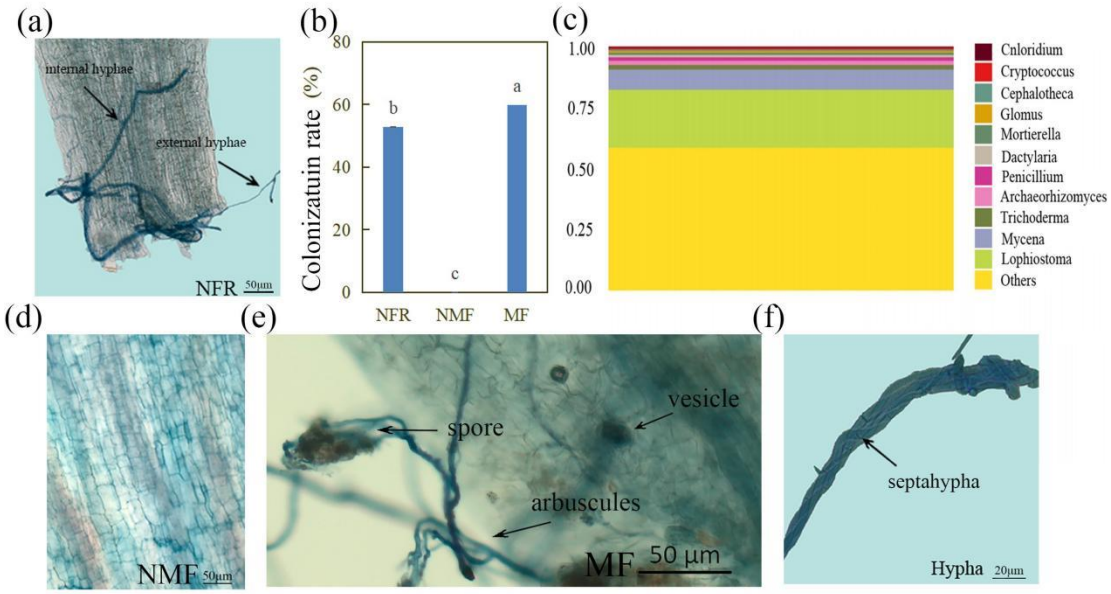

Figure 1. Microscopic observation and molecular identification of mycorrhizal fungi in fine roots collected from the natural forest and seedlings of *C. paliurus*. (**a**) mycorrhizal symbiosis in fine roots collected from the well-growing large trees grown in the natural forest (NFR) of *C. paliurus*; (**b**) colonization rate; (**c**) the molecular identification of fungal richness in fine roots collected from the natural forest of *C. paliurus*; (**d**) colonization observation in fine roots of seedlings without inoculation with mycorrhizal microbial inoculum (NMF); (**e**) colonization observation in fine roots of seedlings inoculated with mycorrhizal microbial inoculum (MF); (**f**) observation of hypha in fine roots of *C. paliurus*. All classifications are at the genera level; the genera of mycorrhizal fungi with abundance less than 0.5% and those with no classification were combined into the Other group.

The mixture of fine root segments and rhizosphere soil was used as the mycorrhizal microbial inoculum for infecting the aseptic seedlings of *C. paliurus*. After 5 months of inoculation, the fine roots of *C. paliurus* seedlings were collected for colonization rate investigation. In this study, the roots of the seedlings in the test group were successfully inoculated with mycorrhizal fungi, as shown by the abundant symbiotic structures in the fine roots of seedlings, while we did not observe any visible mycorrhizal symbiotic structure in the roots of the control group (mycorrhizal microbial inoculum sterilized by autoclave) (Figure 1d–f). The colonization rate of the inoculation group was 59.7%, which was slightly higher than that in the natural forest of *C. paliurus* (Figure 1b). In a previous study, the mixture of fine root segments and rhizosphere soil collected from a 10-year-old walnut plantation was used for infecting current-year walnut (*Juglans regia*) seedlings, which led to an 80.67% colonization rate and a spore density of 21 spores per gram of air-dried rhizosphere soil [28]. These results suggested that the mixture of fine root and rhizosphere soil collected from the natural forest of *C. paliurus* (Wanfoshan, Anhui, China) can be used as the mycorrhizal microbial inoculum to infect seedlings of artificially cultivated *C. paliurus*.

3.2. Variation in Growth and Biomass Accumulation

After one month of inoculation, the height and ground diameter of seedlings were investigated monthly from July to October. The height and ground diameter growth of *C. paliurus* was significantly facilitated by inoculation of mycorrhizal fungi ($p < 0.05$, Figure 2a,b). As compared to control, the height and ground diameter growth measured in October were increased by 21.3% and 19.7%, respectively. In addition, the root, stem and total biomass accumulation were also significantly improved by mycorrhizal fungi inoculation, except for leaf biomass (Figure 2c). Our results are consistent with previous studies in which mycorrhizal plants usually showed a higher shoot biomass, such as *Stevia rebaudiana* and sweet basil (*Ocimum Basilicum*) [29,30]. Indeed, the photosynthetic rate of the inoculation group was significantly increased by 27.0% (Figure 2d), and thus had higher capacity to provide photosynthates for plant growth. Kapoor et al. also showed that plant photosynthetic capacity enhanced after colonization of arbuscular mycorrhiza [17]. The level of 3-indoleacetic acid (IAA), the most abundant and the most important auxins in higher plants, was also increased in mycorrhizal seedlings of *C. paliurus* (Figure 2e). In previous studies, auxin was found to be involved in plant mycorrhizal formation. Both the free and combined IAA levels were increased with the rising colonization rate in mycorrhizal plants [31]. After mycorrhizal inoculation in an auxin signal-insensitive mutant of *dgt* and in a polar-transport hyperactive mutant of *pct*, the colonization rate of these two mutants were decreased compared with that of the wild type [32]. Exogenous auxin analogues 1-naphthylacetic acid (NAA) and 2,4-dichlorophenoxyacetic acid (2,4-D) can promote colonization and symbiotic structure formation of mycorrhizal, and *GH3.4*, encoding indole-3-acetate amide synthase, was also induced [33]. These results indicated that the growth and biomass accumulation of mycorrhizal seedlings of *C. paliurus* were improved through increasing photosynthetic capacity and the level of IAA.

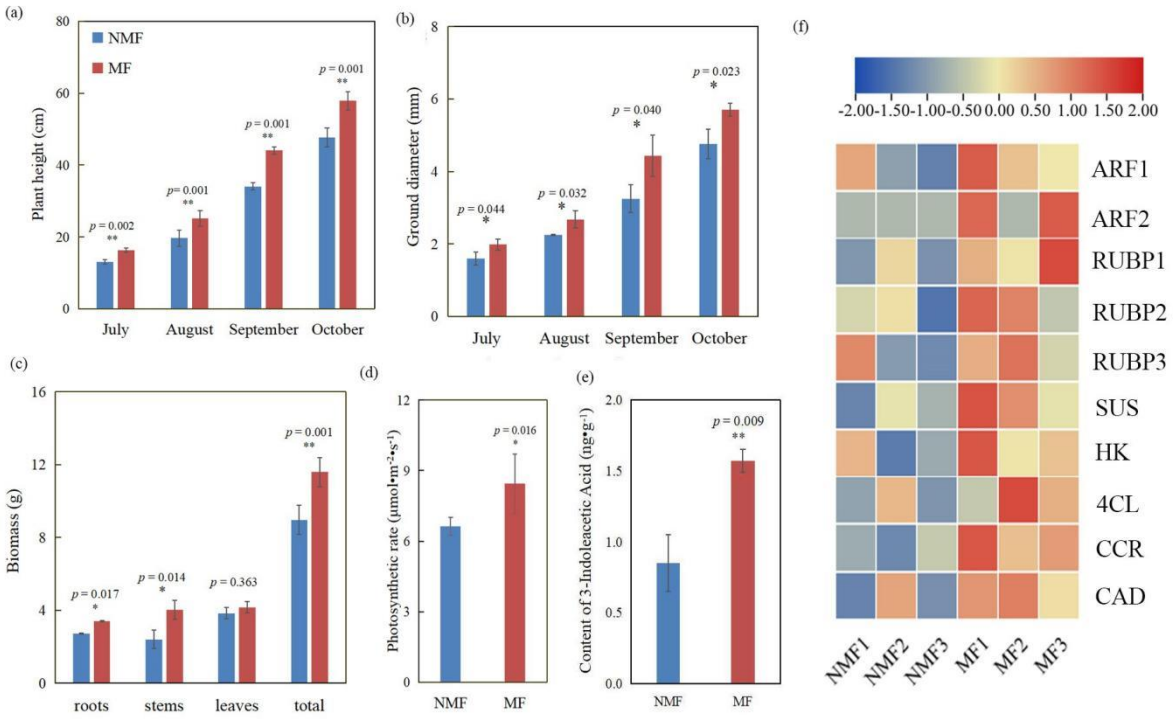

Figure 2. Influence of mycorrhizal fungal colonization on height and ground diameter growth, biomass accumulation, endogenous 3−indoleacetic acid, net photosynthetic rate, and expression of growth−related genes in *C. paliurus*. (**a**,**b**) Changes in plant height and ground diameter after inoculation with mycorrhizal fungi from July to October; (**c**) biomass accumulation in different organs; (**d**,**e**) changes in 3−indoleacetic acid level and net photosynthetic rate in mycorrhizal seedlings or non−mycorrhizal seedlings; (**f**) clustering heat map of the differentially expressed genes (DGEs) in growth−related pathway after inoculation with mycorrhizal fungi. ARF, auxin response factor; RUBP, ribulose−1,5−bisphosphate carboxylase/oxygenase; SUS, sucrose synthase; HK, hexokinase; 4CL, 4−coumarate-CoA ligase; CCR, cinnamoyl−CoA reductase; CAD, cinnamyl alcohol dehydrogenase. * $p < 0.05$ and ** $p < 0.01$ indicate significant differences between inoculation and non-inoculation in two-tailed Student's tests. The color in the heat map represents the corresponding FPKM value of genes.

In addition, transcriptome sequencing was used to comprehensively analyze the effects of mycorrhizal fungal colonization on the expression of growth-related genes in *C. paliurus*. The expression level of two auxin response factors (ARFs), *ARF1* and *ARF2*, were significantly up-regulated (Figure 2f). As transcription factors in the auxin signal transduction pathway, ARFs can specifically bind to auxin response elements (AuxRE) are located in the promoter region of auxin early response genes, regulate the expression of these genes, and ultimately affect plant growth and development [34]. The upregulated levels of auxin content and gene expression of ARFs further indicated the vital role of auxin in the regulation of mycorrhizal fungal colonization and mycorrhizal fungus-mediated plant growth. The genes related to ribulose-1,5-bisphosphate carboxylase/oxygenase (*RUBP1*, *RUBP2*, and *RUBP3*) biosynthesis, the first key enzyme controlling photosynthetic carbon fixation [35], were induced by mycorrhizal fungal colonization, which was in agreement with the increased photosynthetic rate. Plant leaves assimilate carbon dioxide through photosynthesis and synthesize sucrose in the cytoplasm. Indeed, sucrose synthase (SUS) and hexokinase (HK) were induced with the increased photosynthetic capacity in this study. In addition, the enzymatic genes involved in the monolignol biosynthesis pathways were up-regulated, including 4-coumarate-CoA ligase (4CL), cinnamoyl-CoA reductase (CCR), and cinnamyl alcohol dehydrogenase (CAD), which indicated that lignin biosynthesis was induced by mycorrhizal fungal colonization (Figure 2f). Alaux et al. also

found the genes in the lignin biosynthesis pathway of *Solanum tuberosum* were activated by infection of *Phytophthora infestans* [36]. Although lignin belongs to the phenylpropanoid-based polymers, it is necessary for mechanical support for plant growth and the long-distance transportation of water and nutrients [37]. The ectopic lignification and lignin biosynthesis caused by the mutation of *UGT72B1*, which is responsible for the glycosylation of monolignols, were found to lead to growth inhibition [38]. These results demonstrated that facilitation of plant growth induced by mycorrhizal fungal colonization is associated with increased auxin level, photosynthetic capacity, and lignin biosynthesis.

Previous studies have found that plant root morphology, such as higher branch density and biomass accumulation, can be influenced by mycorrhizal fungal colonization [39]. In this study, both root biomass and the number of lateral roots were significantly increased (Figures 2c and 3a–d). However, we did not find any difference between the inoculated and uninoculated mycorrhizal fungi seedlings with regards to the root length of taproots and lateral roots (Figure 3c). In addition, we found an improved mineral nutrient in mycorrhizal seedlings of *C. paliurus*, especially for nitrogen (Figure 3e). Briefly, the levels of nitrogen in leaf and stem, potassium and calcium in stem, and magnesium in root were significantly increased. The previous study also found that mycorrhizal fungi strengthen the ability of the plants to absorb water and nitrogen [38]. Transcription levels of several key enzyme-encoding genes in the nitrogen assimilation pathway were also investigated, including nitrate reductase (NR) and nitrite reductase (NiR) in the nitrate assimilation pathway, as well as glutamine synthetase (GS) and glutamate synthase (GOGAT) in the ammonium assimilation pathway. It was found that the expression of these genes was significantly induced by mycorrhizal fungal colonization (Figure 3f). In the past few decades, mycorrhizal fungi-mediated improved mineral nutrients have been well represented to positively influence the plant growth, which was mainly due to the expanded mycorrhizal fungi mycelia enhancing the ability of plants to obtain water and nutrients from the environment [39–41]. Interestingly, the difference in total phosphorus content between the two groups was not statistically significant. The difference between the present and the previous results may be due to the culture substrate used in this study as it mainly consisted of topsoil collected from the nursery garden, which is rich in organic matter and soil nutrients.

Importantly, the expression of target of rapamycin (TOR) was upregulated, suggesting that growth of mycorrhizal seedlings of *C. paliurus* was induced (Figure 3f). Usually, nutrient-dependent growth of the plant relies on the efficient communication between nutrient acquisition and internal nutrient sensing molecules such as TOR [42]. Meticulous work has confirmed a central role for the TOR kinase in the regulation of plant metabolism, development and stress. It has highly conserved functions in the direct control of protein synthesis, growth processes and autophagy in all eukaryotes, and, in plants, appears to integrate macronutrient, glucose, light, phytohormone (notably auxin) signaling [43]. In response to nutrient deficiency, the TOR kinase inhibits growth and biomass accumulation [43]. Indeed, the nitrogen assimilation, plant growth and biomass accumulation were induced by mycorrhizal fungal colonization. These results indicated that plant growth and biomass accumulation of *C. paliurus* could be synergistically improved by mycorrhizal fungi from the aspects of root morphology, molecular expression, photosynthetic production, mineral nutrient absorption, and endogenous hormones.

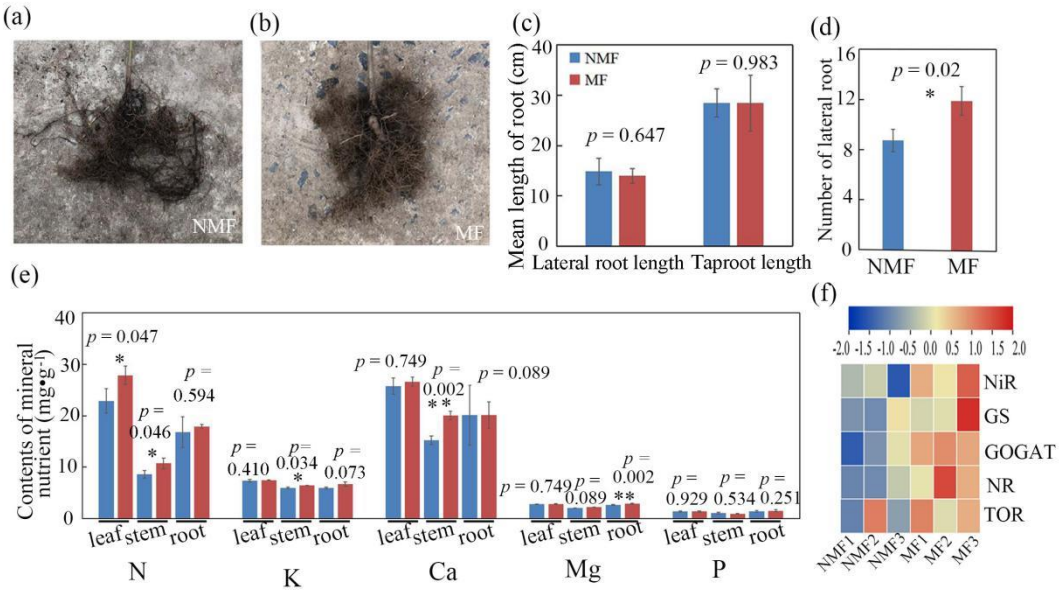

Figure 3. Influence of mycorrhizal fungal colonization on root traits and mineral nutrients in *C. paliurus*. (**a**,**b**) the root picture of inoculated and non−inoculated seedings; (**c**,**d**) the mean length and number of roots; (**e**) changes of mineral nutrients after inoculation with mycorrhizal fungi; the total content of nitrogen (N), potassium (K), calcium (Ca), magnesium (Mg), and phosphors (P) were measured; (**f**) clustering heat map of the DGEs in nitrogen assimilation pathway. NR, nitrate reductase; NiR, nitrite reductase; GS, glutamine synthetase; GOGAT, glutamate synthase; TOR, target of rapamycin. * $p < 0.05$ and ** $p < 0.01$ indicate significant differences between inoculation and non-inoculation in two-tailed Student's tests. The color in the heat map represents the corresponding FPKM value of genes.

3.3. Variation in Secondary Metabolism within Plants

C. paliurus is an important medicinal and edible plant containing various secondary metabolites (flavonoids and triterpenoids) with significant health benefits. The main cultivation goal of medicinal plants is to improve the biosynthesis and accumulation of secondary metabolism, which is an important way to improve the quality of raw materials. In the present study, mycorrhizal fungi were used to infect the aseptic seedlings of *C. paliurus*, and we sought to determine whether the main secondary metabolites could be induced by mycorrhizal fungal colonization. Although the mycorrhizal seedlings of *C. paliurus* possessed a higher content of total flavonoid and total triterpenoid, the differences were not statistically significant, except for total triterpenoid in the stem (Figure 4a,b). In addition, the individual secondary metabolites were isolated, identified and quantified by HPLC-Q-TOF-MS according to the method described by Cao et al. [26]. Our results indicated that 12 out of the 21 compounds were identified in leaves of *C. paliurus* (Figure 4c). Of these compounds, 3-*O*-caffeoylquinic acid and 4-*O*-caffeoylquinic acid belong to the phenolic acid group, quercetin-3-*O*-glucuronide, quercetin-3-*O*-galactoside, kaempferol-3-*O*-glucuronide, kaempferol-3-*O*-glucoside, and kaempferol-3-*O*-rhamnoside are assigned to the flavonoid group, while arjunolic acid, cyclocaric acid B, pterocaryoside A, pterocaryoside B, and oleanolic acid belong to triterpenoid group. However, the other nine compounds of isoquercitrin, quercetin-3-*O*-rhamnoside, 4,5-di-*O*-caffeoylquinic acid, cyclocarioside J, hederagenin, kaempferol-3-(6″-(Z)-cinnamylglucoside), cyclocarioside II, cyclocarioside III, and one unknown compound were not detected in this study. Among them, eight out of 12 compounds—including one phenolic acid, three flavonoids, and four triterpenoids—were significantly induced by mycorrhizal fungal colonization, while the other compounds were not significantly influenced. The six compounds in the stem—3-*O*-caffeoylquinic acid, 4-*O*-caffeoylquinic acid, quercetin-3-*O*-glucuronide, quercetin-3-*O*-galactoside, kaempferol-3-*O*-glucuronide, and oleanolic acid—were not significantly influenced by mycorrhizal

fungi (Figure 4d). For secondary metabolites in the root, kaempferol-3-*O*-glucuronide and oleanolic acid were significantly induced by mycorrhizal fungi, while the other three compounds, 3-*O*-caffeoylquinic acid, quercetin-3-*O*-glucuronide, and quercetin-3-*O*-galactoside, did not change significantly (Figure 4e). Our results indicated that secondary metabolites were mainly accumulated in leaves of *C. paliurus*, and these compounds can be induced by mycorrhizal fungal colonization, especially in leaves and roots.

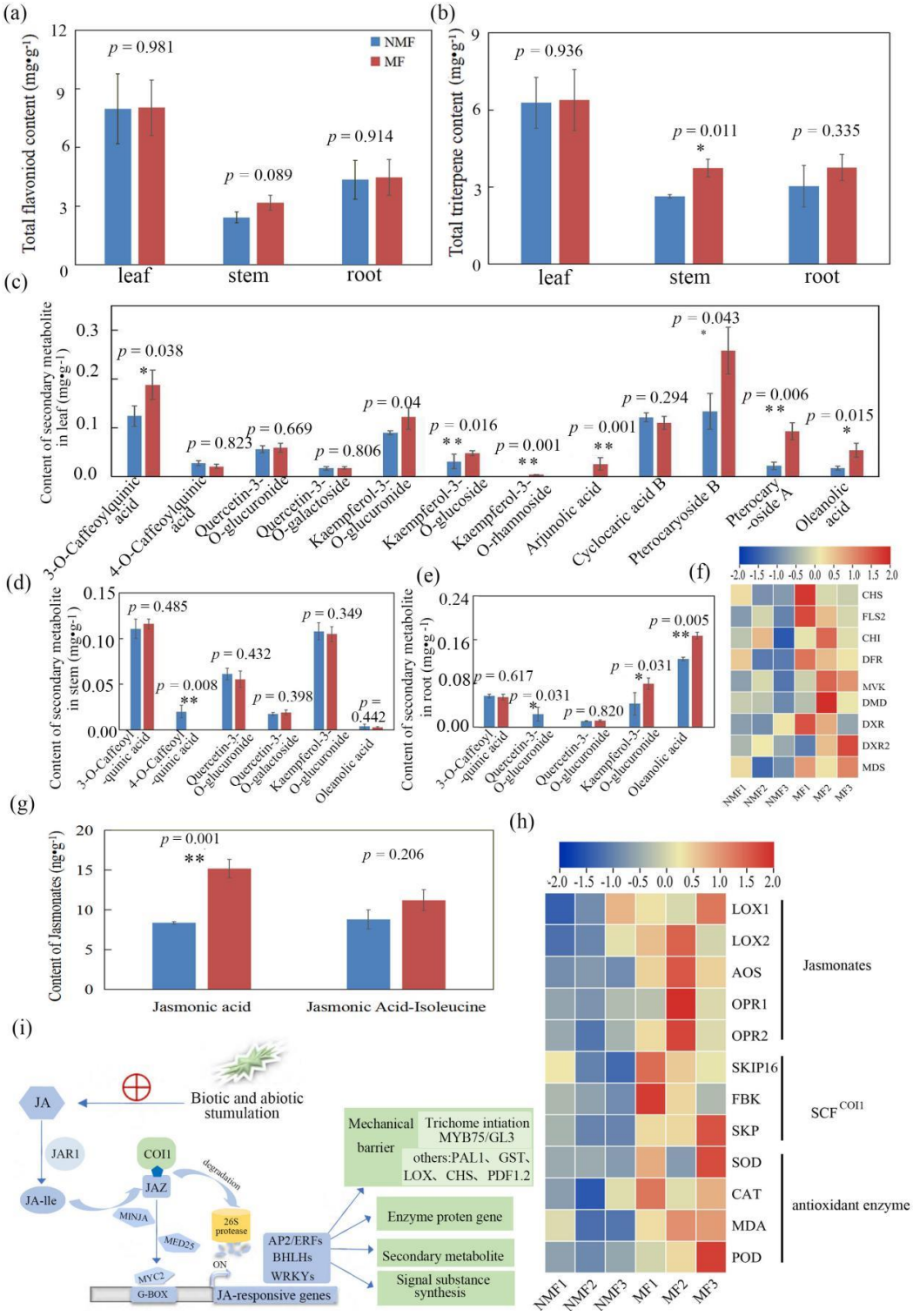

Figure 4. Influence of mycorrhizal fungal colonization on accumulation of secondary metabolites in different organs of *C. paliurus*. (**a**,**b**) the content of total flavonoid and total triterpene in different

organs; (**c**–**e**) the content of individual secondary metabolites in leaves, stems and roots, respectively; (**f**) the expression level of genes involved in the biosynthetic pathways of flavonoid and terpenoid. The key genes in flavonoid pathway include chalcone synthase (CHS), flavonol synthase (FLS), chalcone isomerase (CHI) and Dihydroflavonol 4−reductase (DFR), while key genes in the terpenoids pathway include Mevalonate kinase (MVK), Diphosphomevalonate decarboxylase (DMD), 1−deoxy−D−xylulose−5−phosphate synthase (DXR) and 2−C−methyl−D−erythritol 2,4−cyclodiphosphate synthase (MDS); (**g**) the level of jasmonates; (**h**) the JA defense induced by mycorrhizal fungi; (**i**) the expression level of genes involved in the jasmonic acid signaling and antioxidant systems. The key genes in jasmonic acid signaling include Lipoxygenase (LOX), Allene oxide synthase (AOS) and 12-oxophytodienoate reductase (OPR), S−phase kinase−associated protein 1 (SKP1), and two F−box protein of F−box/kelch−repeat protein (FBK) and F−box protein SKIP 16 (SKIP16). The key genes in antioxidant systems include Superoxide Dismutase (SOD), Catalase (CAT), Malondialdehyde (MDA) and Peroxidase (POD). * $p < 0.05$ and ** $p < 0.01$ indicate significant differences between inoculation and non-inoculation in two-tailed Student's tests.

Given the higher levels of secondary metabolites accumulated in mycorrhizal seedlings of *C. paliurus*, we investigated the gene expression in flavonoid and terpenoid synthetic pathways. In this study, chalcone synthase (CHS), chalcone isomerase (CHI), flavonol synthase and dihydroflavonols 4-reductase (DFR), which are associated with flavonoid biosynthesis, were significantly up-regulated by mycorrhizal fungal colonization (Figure 4f). Among them, CHS is the gateway enzyme of flavonoid biosynthesis, acting on *p*-coumaroyl-CoA as a substrate to generate chalcone, and directs the metabolic flux from the general phenylpropanoid metabolism to flavonoid metabolism [37]. Mutation of CHS in *tt4*, and CHI in *tt5* led to a colorless seed coat [44,45]. Flavonols such as quercetin and kaempferol, the main monomers of flavonoid in *C. paliurus*, were synthesized through the catalysis of FLS. In brief, the induced CHS, CHI, FLS, and DFR resulted in a higher flavonoid accumulation in mycorrhizal seedlings of *C. paliurus*. For triterpenoid biosynthesis in *C. paliurus*, mevalonate kinase (MVK) and mevalonate diphosphate decarboxylase (MVD) (in the mevalonic acid (MVA) pathway), and 1-deoxy-D-xylulose-5-phosphate synthase (DXS) and 2-C-methyl-D-erythritol 2,4-cyclodiphosphate synthase (MDS) (belonging to the methylerythritol phosphate (MEP) pathway), were up-regulated, which suggesting these two biosynthetic pathways of terpenoid were induced by mycorrhizal fungi (Figure 4f). In the MVA pathway, mevalonate (MVA) is catalyzed by a series of enzymes such as MVK, phosphomevalonate kinase (PMK) and MVD to generate isopentenyl-PP (IPP), which is the central precursor of biosynthesis of all terpenoids [46]. In addition, IPP can also be synthesized through the MEP pathway, which usually occurs in chloroplasts and plastids. Analysis of transcriptional expression revealed that both flavonoids and triterpenoids were induced by mycorrhizal fungal colonization, which agreed with the higher levels of secondary metabolites in mycorrhizal seedlings.

As sessile organisms, plants have evolved and obtained diverse strategies for promoting plant stress resistance; these include morphological plasticity and changes in physiological metabolism such as the improved secondary metabolism, biosynthesis of phytohormones associated with stress resistance (e.g., ABA and JA), accumulation of osmotic adjustment substances (e.g., soluble sugar and proline), and activated activity of antioxidant enzymes [37]. For example, flavonoids can be characterized as the scavenger in plants in response to abiotic stresses and function as antioxidants to reduce oxidative damage [47]. In this study, infection of roots by mycorrhizal fungi induced the accumulation of flavonoids and triterpenoids in leaves of *C. paliurus*, indicating that root colonization activated the overall plant defense response. Therefore, the long-distance signal substrate related to stress response was investigated. Previous studies have found that jasmonates (JAs) such as jasmonic acid, methyl jasmonate and jasmonic acid-isoleucine can be facilitated by mycorrhizal fungal colonization, and this plays an important role in mycorrhizal fungi-mediated plants stress resistance [48]. Indeed, the levels of jasmonic acid and jasmonic acid-isoleucine in mycorrhizal seedlings of *C. paliurus* were facilitated, although the

latter was not statistically significant (Figure 4g). The expression of genes encoding the key enzymes in the jasmonic acid biosynthesis pathway, including lipoxygenases (LOX), allene oxide synthase (AOS), and 12-oxophytodienoate reductase (OPR), were induced (Figure 4h). In addition, the expression of indexes reflecting stress or damage of plants, such as malondialdehyde (MDA), superoxide dismutase (SOD), peroxidase (POD), and catalase (CAT), were also upregulated (Figure 4h), which further proved that mycorrhizal plants suffer larger oxidative stress due to the infection of mycorrhizal fungi.

The colonization process of mycorrhizal fungi and the systemic defense in response to colonization have been comprehensively studied. Mycorrhizal fungi, which evolved from diverse types of saprophytic fungi, can secrete carbohydrate-active enzymes such as cellobiohydrolase that function to degrade crystalline cellulose, and lytic polysaccharide monooxygenases [13]. During the colonization, the epidermal cells of plant roots are firstly decomposed, and subsequently the mycelium penetrates into the intercellular or intracellular region of cortical cells and forms the symbiotic structures. When mycorrhizal fungi infect the epidermal cells of plant roots, the defense response is similar to that of biotrophic pathogens, in which fungi are recognized by plant immune systems and then trigger salicylic acid-defense and systemic acquired resistance [49]. In mycorrhizal plants, however, the salicylic acid-mediated defense responses are present only in the early stage of mycorrhizal fungal colonization. When the plant–fungus symbiotic association is established, the later stage of the defense response is mainly mediated by jasmonic acid [50]. The signal transduction pathway of jasmonic acid-mediated defense response has been relatively well understood. In brief, stress signals promote the transformation of the increased jasmonic acid into jasmonic acid-isoleucine and specifically binds to coronatine-insensitive 1 (COI1), and then the jasmonate ZIM-domain (JAZ) repressor proteins are targeted by SCF-type E3 ubiquitin ligase SCFCOI1 (Figure 4i). Finally, JAZ repressor proteins are degraded under the action of the 26S proteasome, and the transcription factors that interact with JAZ repressor proteins are released to initiate the transcription of jasmonic acid-responsive defense genes, such as the biosynthesis of secondary metabolites and defense protein, activation of antioxidant enzymatic activities, and formation of mechanical defense structures [51,52]. Indeed, the expression of genes coding the subunit of SCFCOI1, including the S-phase kinase-associated protein 1 (SKP1), and two F-box proteins of F-box/kelch-repeat protein (FBK) and F-box protein SKIP 16 (SKIP16), were induced by mycorrhizal fungal colonization (Figure 4h). Overall, the facilitated jasmonates, jasmonic acid signal transduction, and secondary metabolism in response to colonization of mycorrhizal fungi suggested that the biosynthesis of flavonoids and triterpenoid in mycorrhizal seedlings of *C. paliurus* could be mediated by jasmonic acid. However, future more systematic analyses should further reveal the roles of the jasmonate-mediated defense response and its function in regulating secondary metabolite biosynthesis.

3.4. Variation in Yield of Secondary Metabolites per Plants

On the basis of the biomass accumulation and the contents of secondary metabolites, the yield of secondary metabolites in different organs per plant was calculated. Among the 12 detected secondary metabolites in leaves of *C. paliurus*, the yield of 3-*O*-caffeoylquinic acid, kaempferol-3-*O*-glucuronide, kaempferol-3-*O*-glucoside, kaempferol-3-*O*-rhamnoside, arjunolic acid, pterocaryoside A, pterocaryoside B, and oleanolic acid were significantly increased, with an increasing rate from 9.8% to 360.5% (Figure 5a). However, we found different infecting effects on various type of secondary metabolites. Compared with phenolic acids and flavonoids, triterpenoid accumulated in leaves was more greatly induced by mycorrhizal fungal colonization. For different type of flavonoids, kaempferol glycosides were more greatly induced than quercetin glycosides. The differential regulation of mycorrhizal fungal colonization on different monomers requires further study. In addition, the yield of 3-*O*-caffeoylquinic acid, quercetin-3-*O*-glucuronide, quercetin-3-*O*-galactoside, and kaempferol-3-*O*-glucuronide in stems, and the yield of kaempferol-3-*O*-glucuronide in roots, were significantly facilitated (Figure 5b,c). The overall mean yield of secondary

metabolites accumulated in the leaves, stems and roots of mycorrhizal seedlings increased by 68.6%, 51.8%, and 63.0% compared to the control group, respectively.

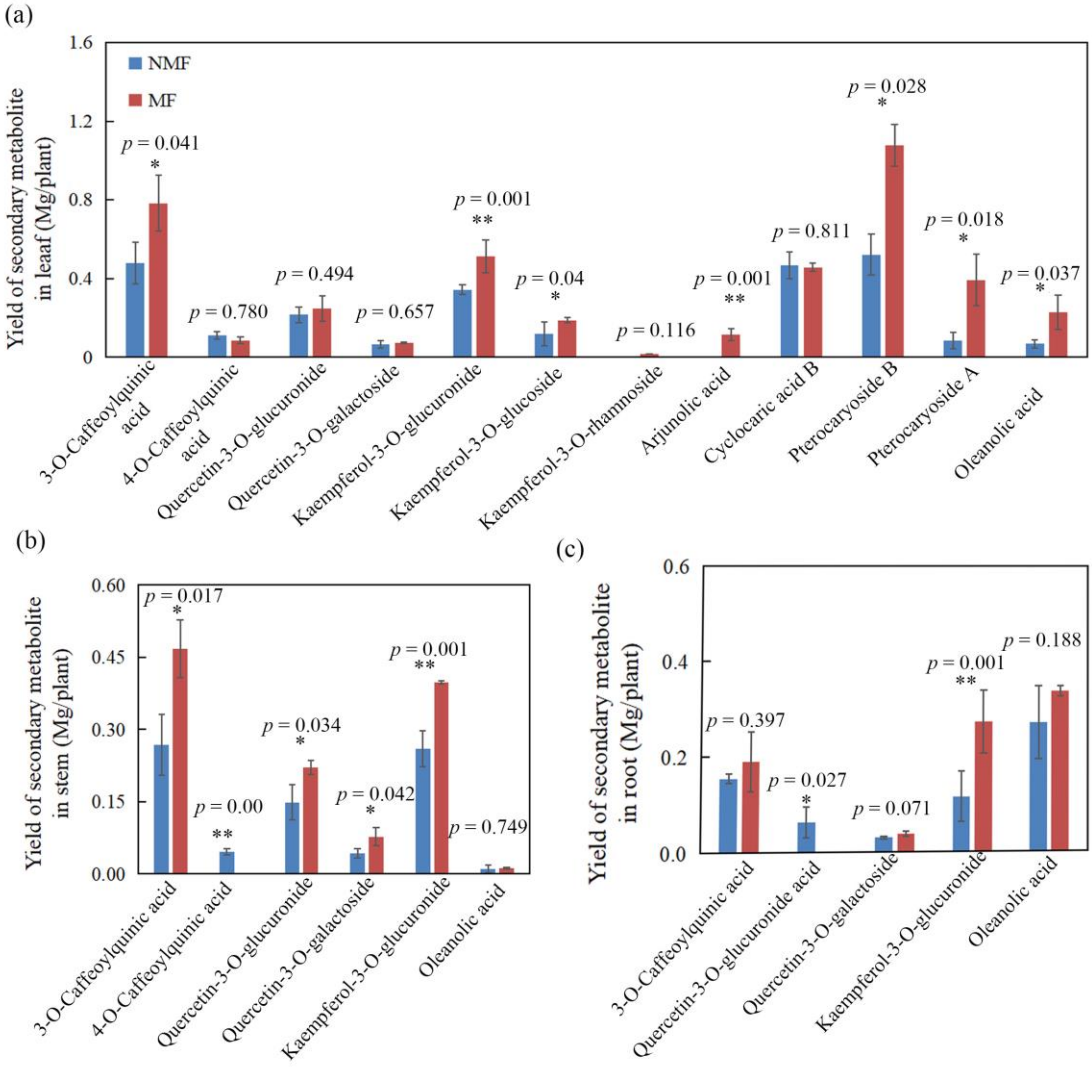

Figure 5. Influence of mycorrhizal fungal colonization on the yield of secondary metabolites per plant. (**a**–**c**) the yield of secondary metabolites in leaves, stems, and roots, respectively. * $p < 0.05$ and ** $p < 0.01$ indicate significant differences between inoculation and non-inoculation in two-tailed Student's tests.

In our previous studies, we found that accumulation of flavonoids in *C. paliurus* was inhibited under the high level of inorganic NPK fertilizer (15% N, 15% P_2O_5, and 15% K_2O) application, while plant growth was improved [5]. Applying nitrogen and phosphate fertilizer alone, we also found a trade-off between secondary metabolism and plant growth; the highest biomass accumulation occurred at high nitrogen levels but this did not lead to the highest flavonoid yield per plant [6–8]. Several hypotheses have been proposed to explain the potential trade-off between secondary metabolism and growth. Among them, the carbon/nutrient balance (CNB) hypothesis assumes that carbon gain and growth depend on the mineral nutrient reserves, i.e., that carbon is allocated to growth whenever the supply of mineral nutrients is adequate, and that carbon accumulated beyond the level used for growth is allocated to defense or storage [53]. These results indicated that the trade-off between growth and secondary metabolism/defense is universal in the fplant kingdom, especially when it comes to soil nutrients and solar radiation, which can promote plants to adapt to the changing environments.

In the past few decades, plant ecologists have focused on the potential trade-off result between growth and defense for studying plant-pathogens relationships [54]. This phenomenon is also an important aspect for cultivation of medicinal plants and crops. In the artificial cultivation practice of medicinal plants, we pay more attention to the balance between secondary metabolite accumulation and plant growth, which is related not only to the quality of raw materials but also to obtaining the greatest harvest yield of target products. Therefore, understanding how environmental factors impact the accumulation of secondary metabolites and plant growth will be of great importance for optimizing cultivation techniques to maintain the quality of raw materials while still keeping a high yield of target phytochemicals. In this study, both growth and accumulation of secondary metabolites of *C. paliurus* were induced by mycorrhizal fungal colonization, which further improved the yield of secondary metabolites per plant. However, how plant growth and secondary metabolisms are synergistically regulated remains largely unknown. Here, we propose a working model for simultaneously enhancing plant growth and secondary metabolism, and further improving production of secondary metabolism in a unit area through inoculating mycorrhizal fungi (Figure 6). In brief, the improved growth of mycorrhizal seedlings was associated with the facilitated endogenous auxin, photosynthesis, development of lateral roots and mineral nutrient absorption (especially for nitrogen). In addition, colonization of mycorrhizal fungi induces a systemic defense response in plants, such that the jasmonic acid biosynthesis and signaling pathways were induced and the biosynthesis of secondary metabolites and antioxidant systems were upregulated. However, further systematic analyses are needed to reveal the roles of jasmonate-mediated secondary metabolite biosynthesis, and its potential function of balancing mycorrhizal fungal infection and growth benefits. These results provide a basis for optimizing the silvicultural system of *C. paliurus* to efficiently produce health-promoting substances for the medicinal and food industries.

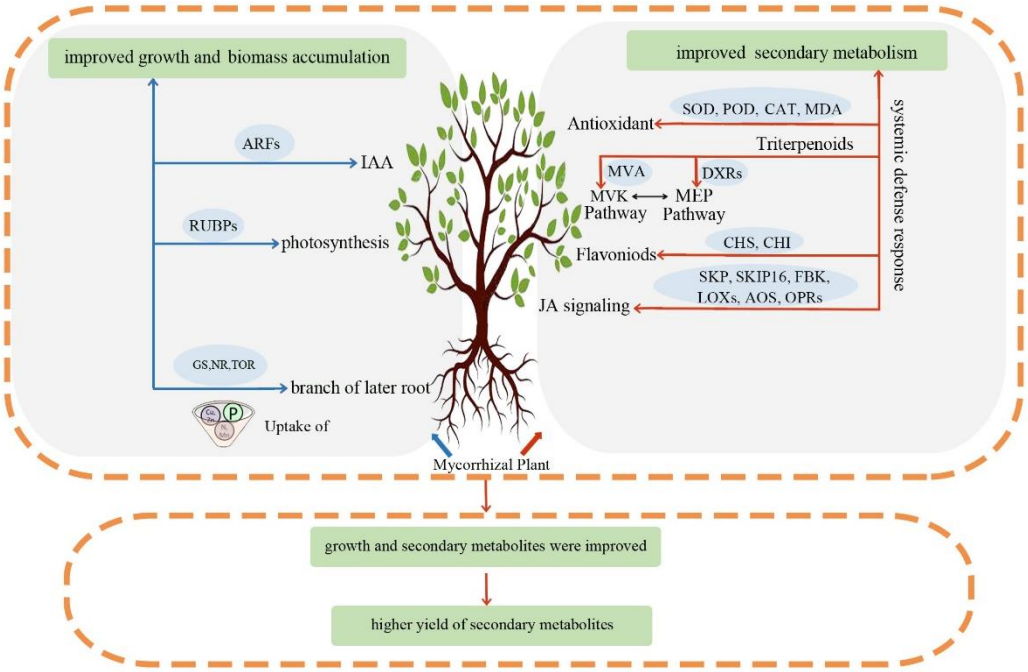

Figure 6. Proposed working model of the role of mycorrhizal fungal in the regulation of growth and secondary metabolites in *C. paliurus*.

4. Conclusions

Overall, plant growth, accumulation of secondary metabolites, and the yield of secondary metabolites per plant were induced by mycorrhizal fungal colonization. The nitrogen absorption, endogenous auxin, net photosynthetic rate, and growth-related genes

were significantly improved in mycorrhizal seedlings of *C. paliurus*, which resulted in significantly higher growth and biomass accumulation. On the other hand, mycorrhizal fungal colonization led to a systemic defense response. Importantly, the jasmonate signal transduction pathway may play a vital role in initiating plant defenses against mycorrhizal fungi and activating secondary metabolism. However, further systematic analyses are needed to reveal the roles of jasmonate-mediated secondary metabolite biosynthesis and its potential function of balancing mycorrhizal fungal infection and growth benefits. The improved growth and accumulation of secondary metabolites further facilitated the yield of health-promoting substrates per plant. Overall, mycorrhizal fungal colonization had a significant positive effect both on plant growth and production of secondary metabolites in leaves of *C. paliurus*. The present study can provide the basis for overcoming the limitations of soil nutrient regulation in cultivation practice and offer a simpler alternative to improve the quality of medicinal plants.

Author Contributions: Conceptualization, T.Z. and B.D.; investigation, T.Z., B.Y., M.Z. and S.C.; data curation, T.Z. and S.C.; formal analysis, T.Z., B.Y. and B.D.; writing—original draft, T.Z.; writing—editing and review, B.Y., M.Z., S.C. and B.D.; visualization, B.D.; resources, B.D.; methodology, T.Z. and B.D.; funding acquisition, B.D.; supervision, B.D. All authors have read and agreed to the published version of the manuscript.

Funding: This study was funded by National Natural Science Foundation of China, grant number No. 31800528, and the Innovation Fund Designated for Forestry Science of Anhui Provence.

Acknowledgments: We thank Bo Huang and Hui Zhang, of Anhui Agricultural University, for their contributions to this work.

Conflicts of Interest: The authors declare no conflict of interest.

References

1. Fang, S.; Yang, W.; Chu, X.; Shang, X.; She, C.; Fu, X. Provenance and temporal variations in selected flavonoids in leaves of *Cyclocarya paliurus*. *Food Chem.* **2011**, *124*, 1382–1386. [CrossRef]
2. Lin, Z.; Wu, Z.-F.; Jiang, C.-H.; Zhang, Q.-W.; Ouyang, S.; Che, C.-T.; Zhang, J.; Yin, Z.-Q. The chloroform extract of *Cyclocarya paliurus* attenuates high-fat diet induced non-alcoholic hepatic steatosis in Sprague Dawley rats. *Phytomedicine* **2016**, *23*, 1475–1483. [CrossRef] [PubMed]
3. Wang, Q.; Jiang, C.; Fang, S.; Wang, J.; Ji, Y.; Shang, X.; Ni, Y.; Yin, Z.; Zhang, J. Antihyperglycemic, antihyperlipidemic and antioxidant effects of ethanol and aqueous extracts of *Cyclocarya paliurus* leaves in type 2 diabetic rats. *J. Ethnopharmacol.* **2013**, *150*, 1119–1127. [CrossRef] [PubMed]
4. Wu, Z.F.; Gao, T.H.; Zhong, R.L.; Lin, Z.; Jiang, C.H.; Ouyang, S.; Zhao, M.; Che, C.T.; Zhang, J.; Yin, Z.Q. Antihyperlipidaemic effect of triterpenic acid-enriched fraction from *Cyclocarya paliurus* leaves in hyperlipidaemic rats. *Pharm. Boil.* **2017**, *55*, 712–721. [CrossRef] [PubMed]
5. Deng, B.; Shang, X.; Fang, S.; Li, Q.; Fu, X.; Su, J. Integrated Effects of Light Intensity and Fertilization on Growth and Flavonoid Accumulation in *Cyclocarya paliurus*. *J. Agric. Food Chem.* **2012**, *60*, 6286–6292. [CrossRef] [PubMed]
6. Deng, B.; Li, Y.; Lei, G.; Liu, G. Effects of nitrogen availability on mineral nutrient balance and flavonoid accumulation in *Cyclocarya paliurus*. *Plant Physiol. Biochem.* **2019**, *135*, 111–118. [CrossRef]
7. Deng, B.; Li, Y.; Xu, D.; Ye, Q.; Liu, G. Nitrogen availability alters flavonoid accumulation in *Cyclocarya paliurus* via the effects on the internal carbon/nitrogen balance. *Sci. Rep.* **2019**, *9*, 2370. [CrossRef]
8. Zhang, X.; Zhang, M.; Zhao, T.; Deng, B. Phosphate availability regulates flavonoid accumulation associated with photosynthetic carbon partitioning in *Cyclocarya paliurus*. *Physiol. Plant.* **2021**, *173*, 1956–1966. [CrossRef]
9. Brundrett, M.C.; Tedersoo, L. Evolutionary history of mycorrhizal symbioses and global host plant diversity. *New Phytol.* **2018**, *220*, 1108–1115. [CrossRef]
10. Mandal, S.; Upadhyay, S.; Singh, V.P.; Kapoor, R. Enhanced production of steviol glycosides in mycorrhizal plants: A concerted effect of arbuscular mycorrhizal symbiosis on transcription of biosynthetic genes. *Plant Physiol. Biochem.* **2015**, *89*, 100–106. [CrossRef]
11. Mandal, S.; Upadhyay, S.; Wajid, S.; Ram, M.; Jain, D.C.; Singh, V.P.; Abdin, M.Z.; Kapoor, R. Arbuscular mycorrhiza increase artemisinin accumulation in *Artemisia annua* by higher expression of key biosynthesis genes via enhanced jasmonic acid levels. *Mycorrhiza* **2015**, *25*, 345–357. [CrossRef]
12. Sheteiwy, M.S.; Elgawad, H.A.; Xiong, Y.; Macovei, A.; Brestic, M.; Skalicky, M.; Shaghaleh, H.; Hamoud, Y.A.; El-Sawah, A.M. Inoculation with Bacillus amyloliquefaciens and mycorrhiza confers tolerance to drought stress and improve seed yield and quality of soybean plant. *Physiol. Plant.* **2021**, *172*, 2153–2169. [CrossRef] [PubMed]

13. Nagy, L.G.; Riley, R.; Tritt, A.; Adam, C.; Daum, C.; Floudas, D.; Sun, H.; Yadav, J.S.; Pangilinan, J.; Larsson, K.-H.; et al. Comparative Genomics of Early-Diverging Mushroom-Forming Fungi Provides Insights into the Origins of Lignocellulose Decay Capabilities. *Mol. Biol. Evol.* **2016**, *33*, 959–970. [CrossRef] [PubMed]
14. Plett, J.M.; Daguerre, Y.; Wittulsky, S.; Vayssières, A.; Deveau, A.; Melton, S.J.; Kohler, A.; Morrell-Falvey, J.L.; Brun, A.; Veneault-Fourrey, C.; et al. Effector MiSSP7 of the mutualistic fungus *Laccaria bicolor* stabilizes the *Populus* JAZ6 protein and represses jasmonic acid (JA) responsive genes. *Proc. Natl. Acad. Sci. USA* **2014**, *111*, 8299–8304. [CrossRef] [PubMed]
15. Park, J.-H.; Halitschke, R.; Kim, H.B.; Baldwin, I.T.; Feldmann, K.A.; Feyereisen, R. A knock-out mutation in allene oxide synthase results in male sterility and defective wound signal transduction in *Arabidopsis* due to a block in jasmonic acid biosynthesis. *Plant J.* **2002**, *31*, 1–12. [CrossRef] [PubMed]
16. Gutjahr, C. Phytohormone signaling in arbuscular mycorrhiza development. *Curr. Opin. Plant Biol.* **2014**, *20*, 26–34. [CrossRef] [PubMed]
17. Kapoor, R.; Anand, G.; Gupta, P.; Mandal, S. Insight into the mechanisms of enhanced production of valuable terpenoids by arbuscular mycorrhiza. *Phytochem. Rev.* **2017**, *16*, 677–692. [CrossRef]
18. Le Roy, J.; Huss, B.; Creach, A.; Hawkins, S.; Neutelings, G. Glycosylation is a major regulator of phenylpropanoid availability and biological activity in plants. *Front. Plant Sci.* **2016**, *7*, 735. [CrossRef]
19. Augustin, J.M.; Drok, S.; Shinoda, T.; Sanmiya, K.; Nielsen, J.K.; Khakimov, B.; Olsen, C.E.; Hansen, E.H.; Kuzina, V.; Ekstrøm, C.T.; et al. UDP-Glycosyltransferases from the UGT73C Subfamily in *Barbarea vulgaris* Catalyze Sapogenin 3-O-Glucosylation in Saponin-Mediated Insect Resistance. *Plant Physiol.* **2012**, *160*, 1881–1895. [CrossRef]
20. Nielsen, J.K.; Nagao, T.; Okabe, H.; Shinoda, T. Resistance in the Plant, *Barbarea vulgaris*, and Counter-Adaptations in Flea Beetles Mediated by Saponins. *J. Chem. Ecol.* **2010**, *36*, 277–285. [CrossRef]
21. Fang, S.; Wang, J.; Wei, Z.; Zhu, Z. Methods to break seed dormancy in *Cyclocarya paliurus* (Batal)Iljinskaja. *Sci. Hortic.* **2006**, *110*, 305–309. [CrossRef]
22. Zhang, Z.F.; Zhang, J.C.; Zhou, L.W.; Xu, G.P.; Li, Y.Q. Effects of arbuscular mycorrhizal fungi on the growth of afforestation seedlings in a rocky desertification area. *Chin. J. Ecol.* **2018**, *37*, 2917–2934. (In Chinese)
23. Massenssini, A.M.; Bonduki, V.H.A.; Tótola, M.R.; Ferreira, F.A.; Costa, M.D. Arbuscular mycorrhizal associations and occurrence of dark septate endophytes in the roots of Brazilian weed plants. *Mycorrhiza* **2014**, *24*, 153–159. [CrossRef] [PubMed]
24. Bao, J.; Cai, Y.; Sun, M.; Wang, G.; Corke, H. Anthocyanins, flavonols, and free radical scavenging activity of Chinese bayberry (*Myrica rubra*) extracts and their color properties and stability. *J. Agric. Food Chem.* **2005**, *53*, 2327–2332. [CrossRef]
25. Fan, J.-P.; He, C.-H. Simultaneous quantification of three major bioactive triterpene acids in the leaves of *Diospyros kaki* by high-performance liquid chromatography method. *J. Pharm. Biomed. Anal.* **2006**, *41*, 950–956. [CrossRef]
26. Cao, Y.; Fang, S.; Yin, Z.; Fu, X.; Shang, X.; Yang, W.; Yang, H. Chemical fingerprint and multicomponent quantitative analysis for the quality evaluation of *Cyclocarya paliurus* leaves by HPLC–Q–TOF–MS. *Molecules* **2017**, *22*, 1927. [CrossRef]
27. Wu, T.G.; Mitchell, B.M.; Carothers, T.S.; Coats, D.K.; Brady-McCreery, K.M.; Paysse, E.A.; Wilhelmus, K.R. Molecular analysis of the pediatric ocular surface for fungi. *Curr. Eye Res.* **2003**, *26*, 33–36. [CrossRef]
28. Mao, J.; Li, R.; Jing, Y.; Ning, D.; Li, Y.; Chen, H. Arbuscular mycorrhizal fungi associated with walnut trees and their effects on seedling growth. *J. For. Environ.* **2022**, *42*, 71–80. (In Chinese)
29. Mandal, S.; Evelin, H.; Giri, B.; Singh, V.P.; Kapoor, R. Arbuscular mycorrhiza enhances the production of stevioside and rebaudioside-A in *Stevia rebaudiana* via nutritional and non-nutritional mechanisms. *Appl. Soil Ecol.* **2013**, *72*, 187–194. [CrossRef]
30. Rasouli-Sadaghiani, M.; Hassani, A.; Barin, M.; Danesh, Y.R.; Sefidkon, F. Effects of arbuscular mycorrhizal (AM) fungi on growth, essential oil production and nutrients uptake in basil. *J. Med. Plant. Res.* **2010**, *4*, 2222–2228.
31. Fitze, D.; Wiepning, A.; Kaldorf, M.; Ludwig-Müller, J. Auxins in the development of an arbuscular mycorrhizal symbiosis in maize. *J. Plant Physiol.* **2005**, *162*, 1210–1219. [CrossRef] [PubMed]
32. Hanlon, M.; Coenen, C. Genetic evidence for auxin involvement in arbuscular mycorrhiza initiation. *New Phytol.* **2011**, *189*, 701–709. [CrossRef] [PubMed]
33. Liao, D.; Chen, X.; Chen, A.; Wang, H.; Liu, J.; Liu, J.; Gu, M.; Sun, S.; Xu, G. The Characterization of Six Auxin-Induced Tomato GH3 Genes Uncovers a Member, *SlGH3.4*, Strongly Responsive to Arbuscular Mycorrhizal Symbiosis. *Plant Cell Physiol.* **2015**, *56*, 674–687. [CrossRef] [PubMed]
34. Guilfoyle, T.J.; Hagen, G. Auxin response factors. *Curr. Opin. Plant Biol.* **2007**, *10*, 453–460. [CrossRef]
35. Chen, J.; Wang, P.; Mi, H.-L.; Chen, G.-Y.; Xu, D.-Q. Reversible association of ribulose-1, 5-bisphosphate carboxylase/oxygenase activase with the thylakoid membrane depends upon the ATP level and pH in rice without heat stress. *J. Exp. Bot.* **2010**, *61*, 2939–2950. [CrossRef]
36. Genre, A.; Lanfranco, L.; Perotto, S.; Bonfante, P. Unique and common traits in mycorrhizal symbioses. *Nat. Rev. Microbiol.* **2020**, *18*, 649–660. [CrossRef]
37. Dong, N.Q.; Lin, H.X. Contribution of phenylpropanoid metabolism to plant development and plant–environment interactions. *J. Integr. Plant Biol.* **2021**, *63*, 180–209. [CrossRef]
38. Lin, J.-S.; Huang, X.-X.; Li, Q.; Cao, Y.; Bao, Y.; Meng, X.-F.; Li, Y.-J.; Fu, C.; Hou, B.-K. UDP-glycosyltransferase 72B1 catalyzes the glucose conjugation of monolignols and is essential for the normal cell wall lignification in *Arabidopsis thaliana*. *Plant J.* **2016**, *88*, 26–42. [CrossRef]

39. Wu, Q.-S.; Zou, Y.-N.; He, X.-H. Contributions of arbuscular mycorrhizal fungi to growth, photosynthesis, root morphology and ionic balance of citrus seedlings under salt stress. *Acta Physiol. Plant.* **2010**, *32*, 297–304. [CrossRef]
40. Alaux, P.L.; Naveau, F.; Declerck, S.; Cranenbrouck, S. Common mycorrhizal network induced JA/ET genes expression in healthy potato plants connected to potato plants y by *Phytophthora infestans*. *Front. Plant Sci.* **2020**, *11*, 602. [CrossRef]
41. Oliveira, R.S.; Franco, A.R.; Vosatka, M.; Castro, P.M.L. Management of nursery practices for efficient ectomycorrhizal fungi application in the production of *Quercus ilex*. *Symbiosis* **2010**, *52*, 125–131. [CrossRef]
42. Wu, Y.; Shi, L.; Li, L.; Fu, L.; Liu, Y.; Xiong, Y.; Sheen, J. Integration of nutrient, energy, light, and hormone signaling via TOR in plants. *J. Exp. Bot.* **2019**, *70*, 2227–2238. [CrossRef] [PubMed]
43. Crepin, N.; Rolland, F. SnRK1 activation, signaling, and networking for energy homeostasis. *Curr. Opin. Plant Biol.* **2019**, *51*, 29–36. [CrossRef] [PubMed]
44. Shirley, B.W.; Kubasek, W.L.; Storz, G.; Bruggemann, E.; Koornneef, M.; Ausubel, F.M.; Goodman, H.M. Analysis of *Arabidopsis* mutants deficient in flavonoid biosynthesis. *Plant J.* **1995**, *8*, 659–671. [CrossRef] [PubMed]
45. Winkel-Shirley, B. Flavonoid biosynthesis. A colorful model for genetics, biochemistry, cell biology, and biotechnology. *Plant Physiol.* **2001**, *126*, 485–493. [CrossRef]
46. Lv, Z.Y.; Zhang, F.Y.; Pan, Q.F.; Fu, X.Q.; Jiang, W.M.; Shen, Q.; Yan, T.X.; Shi, P.; Lu, X.; Sun, X.F.; et al. Branch pathway blocking in Artemisia annua is a useful method for obtaining high yield artemisnin. *Plant Cell Physiol.* **2016**, *57*, 588–602. [CrossRef]
47. Cui, L.G.; Shan, J.X.; Shi, M.; Gao, J.P.; Lin, H.X. The miR156-SPL 9-DFR pathway coordinates the relationship between development and abiotic stress tolerance in plants. *Plant J.* **2014**, *80*, 1108–1117. [CrossRef]
48. Li, Y.; Liu, Z.; Hou, H.; Lei, H.; Zhu, X.; Li, X.; He, X.; Tian, C. Arbuscular mycorrhizal fungi-enhanced resistance against *Phytophthora sojae* infection on soybean leaves is mediated by a network involving hydrogen peroxide, jasmonic acid, and the metabolism of carbon and nitrogen. *Acta Physiol. Plant.* **2013**, *35*, 3465–3475. [CrossRef]
49. Jung, S.C.; Martinez-Medina, A.; Lopez-Raez, J.A.; Pozo, M.J. Mycorrhiza-Induced Resistance and Priming of Plant Defenses. *J. Chem. Ecol.* **2012**, *38*, 651–664. [CrossRef]
50. Plett, J.M.; Khachane, A.; Ouassou, M.; Sundberg, B.; Kohler, A.; Martin, F. Ethylene and jasmonic acid act as negative modulators during mutualistic symbiosis between *Laccaria bicolor* and *Populus* roots. *New Phytol.* **2014**, *202*, 270–286. [CrossRef]
51. Fonseca, S.; Chico, J.M.; Solano, R. The jasmonate pathway: The ligand, the receptor and the core signaling module. *Curr. Opin. Plant Biol.* **2009**, *12*, 539–547. [CrossRef] [PubMed]
52. Katsir, L.; Chung, H.S.; Koo, A.J.; Howe, G.A. Jasmonate signaling: A conserved mechanism of hormone sensing. *Curr. Opin. Plant Biol.* **2008**, *11*, 428–435. [CrossRef] [PubMed]
53. Stamp, N. Out of the Quagmire of Plant Defense Hypotheses. *Q. Rev. Biol.* **2003**, *78*, 23–55. [CrossRef] [PubMed]
54. Larbat, R.; Robin, C.; Lillo, C.; Drengstig, T.; Ruoff, P. Modeling the diversion of primary carbon flux into secondary metabolism under variable nitrate and light/dark conditions. *J. Theor. Biol.* **2016**, *402*, 144–157. [CrossRef]